CHEMISTRY & BIODIVERSITY

Accepted Article

Title: Design, Synthesis and Molecular Docking Studies of some Tetrahydropyrimidine Derivatives as Possible Fascin Inhibitors

Authors: Narges Riahi, Amirhosein Kefayat, Ahmad Ghasemi, Mohammadhosein Asgarshamsi, Mojtaba Panjehpour, and Afshin Fassihi

To be cited as: *Chem. Biodiversity* 10.1002/cbdv.201800339

Link to VoR: http://dx.doi.org/10.1002/cbdv.201800339

Chem. Biodiversity

Design, Synthesis and Molecular Docking Studies of some Tetrahydropyrimidine Derivatives as Possible Fascin Inhibitors

Narges Riahi,[a] Amirhosein Kefayat,[b] Ahmad Ghasemi,[c] Mohammadhosein Asgarshamsi,[a] Mojtaba Panjehpoor,[d] Afshin Fassihi [a,*]

[a]Department of Medicinal Chemistry, School of Pharmacy and Pharmaceutical Sciences, Isfahan University of Medical Sciences, 81746-73461, Isfahan, Iran

E-mail: fassihi@pharm.mui.ac.ir (A. Fassihi)

[b]Department of Oncology, Cancer Prevention Research Center, Isfahan University of Medical science,81746-73461, Isfahan, Iran.

[c]Department of Basic Medical Sciences, Neyshabur University of Medical Sciences, Neyshabur, Iran.

[d]Department of Biochemistry, School of Pharmacy and Pharmaceutical Sciences, Isfahan University of Medical Sciences, 81746-73461, Isfahan, Iran

Eight derivatives of tetrahydropyrimidine scaffold were designed and prepared as hybrid compounds possessing the structural features of both Monastrol as an anticancer drug and Nifedipine as a Fascin blocking agent. All of the compounds were evaluated for their cytotoxic potency and the ability to inhibit 4T1 breast cancer cells migration. Then they were investigated *in silico* for their ability to inhibit the Fascin protein using molecular docking simulation. The most potent compound was **4d** and the weakest one was **4a** according to the *in vitro* cytotoxicity assay. The corresponding IC_{50} values were 193.70 and 248.75 µmol, respectively. The least cytotoxic compound (**4a**) was one of the strongest ones in binding to the Fascin binding site according to the molecular docking results. **4a** and **4e** inhibited the 4T1 cells migration better than other compounds. They were more potent than Nifedipine in inhibiting the migration process. *In silico* studies proved **4h** to be the most potent Fascin inhibitor in terms of ΔG_{bind} although it was not inhibiting migration. The controversy between the *in vitro* and *in silico* results may cancel the theory of the involvement of the Fascin inhibition in the migration inhibition. However, the considerable anti-migratory effects of some of the synthesized compounds encourage performing further *in vivo* experiments to introduce novel tumor metastasis inhibitors.

Keywords: Tetrahydroprimidines • Fascin • Cytotoxicity • Migration • Molecular Docking

Introduction

Tumor metastasis has been recognized as the dissemination of malignant cells from the primary tissue to distant sites via organ-specific patterns.[1] Progress in the knowledge of tumor invasion has yielded a list of drug targets like enzymes, receptors, and multiple signaling pathways.[2] Now it is known that the process of metastasis consists of sequential and interlinked steps, all of which depend on the hemostasis factors that promote tumor cell proliferation, angiogenesis, migration, invasion and extravasation into organ parenchyma.[3] It seems that local invasion and metastasis of malignant cells are the main features of solid cancer cells. Furthermore, resistance to cytotoxic drugs is attributed to mutations of the target or cell migration and/or invasion which are the main causes of treatment failure. The metastatic process is a promising therapeutic target and many efforts have been invested in the identification of cellular structures involved in the cell migration process.

Filopodia are thin finger-like and highly dynamic actin-rich membrane protrusions that are essential for migration.[4] Filopodia enable migrating cells to navigate their surroundings and determine the direction of migration.[5] Filopodia extend beyond the leading edge of migrating cells and are supported by rigid tightly bonded actin filaments.[6] Fascin is an evolutionarily conserved actin binding protein that is localized in filopodia. This protein with its uniquely folded 4-β-3 foil structure is up-regulated as the part of the program of epithelial to mesenchymal cancer cell progression.[7] Fascin gives special motility and invasion properties to the cancer cells. Based on *in vivo* and *in vitro* conducted model studies, it has been demonstrated that Fascin as a primary molecular biomarker

plays a significant role in tumor progression. Depletion or inhibition of this protein results in reduced cell migration. In contrast, Fascin is up-regulated by the invasion capacity of the cancer cells. Additionally, these alterations provide a target for designing novel agents to inhibit cancer cell migration.[8]

Two major binding sites were recognized for binding activity of Fascin. Each binding site is essential for filopodia formation inside the cells. Some macrocyclic ketones have been recognized that occupy Fascin binding sites and specifically inhibit its biochemical function of filopodia formation induction. These Fascin inhibitors block tumor cell migration and inhibit invasion and metastasis. Migrastatin and its structural analogs are potent Fascin inhibitors of metastatic tumor cell migrations.[9] Some small molecules have also been identified according to a cell based Fascin bioassay as potent Fascin inhibitors. Nifedipine, Baclofen and Amantadine are three examples of these inhibitors.[10] The chemical structures of these compounds are illustrated in Figure **1**.

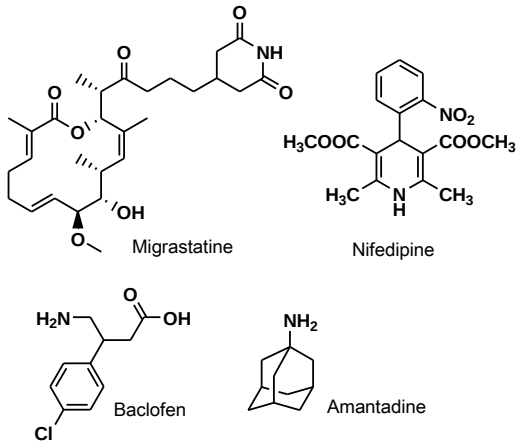

Figure 1. Structures of Migrastatin, Nifedipine, Baclofen and Amantadin

Monastrol is a prototype anticancer drug that selectively inhibits dimeric kinesin Eg5 regulation (Figure **2**). As a tetrahydropyrimidine derivative, Monastrol has a structural similarity to Nifedipine, a dihydropyridine derivative which inhibits Fascine. From the chemical structure point of view, tetrahydropyrimidine scaffold can be regarded as the aza analog of dihydropyridine. Tetrahydropyrimidine and dihydropyridine derivatives have also been identified to have similar pharmacological properties. Calcium channel blocking, anti-tubercular, anti-microbial and anti-cancer activities are some of these shared pharmacological properties.[11]

Effective treatment of solid cancer can be achieved by cytotoxic compounds that are also able to inhibit the ability of cancer cells to invade through the extracellular matrix and establish secondary tumors. Thus, a specific design of hybrid cytotoxic and anti-invasive/antimetastatic compounds for the treatment of solid cancer must not be ignored. Medicinal chemistry efforts based on cell biology and structure-activity relationship have well-defined pharmacophores of promising cytotoxic anti-migrastatic agents in both synthetic and natural sources.[12-14]

In the present study, we aimed at the synthesis of some hybrid tetrahydropyrimidine derivatives possessing the structural features of both Monastrol and Nifedipine. This strategy which is illustrated in Figure **2** may provide the designed molecules biological properties of cytotoxicity and the ability to inhibit tumor cell migration. The anti-migratory activity would be a good additive feature for cytotoxic agents. In fact, this feature would change nothing in the process of the solid cancer treatment with a strong cytotoxic compound; but, in the case of moderate cytotoxic agents those cells which were not destroyed by the compound would not have any chance to migrate which leads to invasion. The designed compounds were prepared in the lab and the cytotoxic effects as well as the migration inhibitory ability of the synthesized compounds were evaluated. All of the compounds were also investigated *in silico* for their abilities to inhibit the Fascin protein using molecular docking simulation.

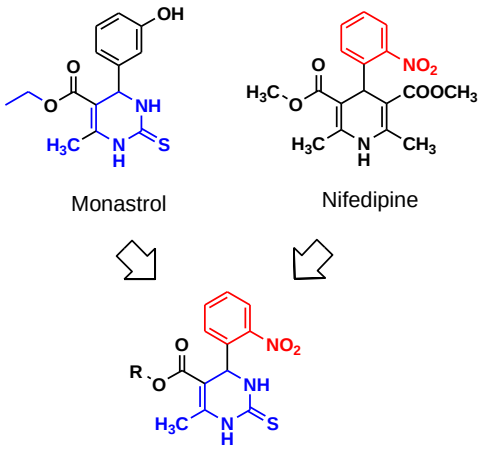

Figure 2. Design of tetrahydropyrimidines with cytotoxic and migration inhibitory activity based on Nifedipin and Monastrol structures

Results and Discussion

Chemistry

Eight 1,2,3,4-tetrahydropyrimidine derivatives (**4a-h**) were synthesized as described in Scheme **1**. General structure and the structural details of the designed compounds are provided in Table **1**.

Table 1. General structure and the structural details of the designed compounds

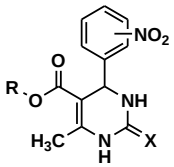

(4a-h)

Compound	Nitro position	R	X
4a	*ortho*	CH_3	O
4b	*ortho*	C_2H_5	O
4c	*meta*	CH_3	O
4d	*meta*	C_2H_5	O
4e	*ortho*	CH_3	S
4f	*ortho*	C_2H_5	S
4g	*meta*	CH_3	S
4h	*meta*	C_2H_5	S

The core 1,2,3,4-tetrahydropyridine ring was constructed according to the Biginelli multicomponent cyclocondensation reaction.[15] In brief, a mixture of the proper aldehyde (**1**,**1'**), alkyl acetoacetate (**2**,**2'**) and urea/thiourea (**3**,**3'**) was refluxed in a suitable solvent using the proper Lewis acid catalyst to provide the **4a-h** products. For compounds **4a-d**, absolute ethanol and cobalt hydrogen sulfate were the solvent and catalyst, respectively. Tetrahydrofuran as the solvent and polyphosphate ester as the Lewis acid catalyst were used for the preparation of **4e-h**. The structures of the title compounds were confirmed by IR and ^{1}H-NMR spectroscopy. Some of the characterization data of the prepared compounds are summarized as follows. All compounds showed in the IR spectra an absorption band at 1662–1716 cm^{-1}, typical of the stretch vibrations belonging to the carboxylate C=O group. The ureide carbonyl or thiocarbonyl groups appeared at 1626–1645 cm^{-1} and 1566-1670 cm^{-1}, respectively. The ^{1}H-NMR spectra of all final compounds contained a singlet in the 2.27–2.30 ppm region due to the CH_3 protons at the C6 position. The characteristic peak for the C4-H of the 1,2,3,4-tetrahydropyrimidine ring appeared at 5.29–5.94 ppm confirming the formation of this heterocycle. It was a singlet peak for **4a-d**, but a doublet (J=2.8-3.6 Hz) for the 2-thiocarbonyl analogues of them, compounds **4e-h**. This doublet appeared as a result of the coupling of C4 proton with the hydrogen attached to N3. It can be explained in this way that in **4a-d**, N3 does not bear the proton all the times as a consequence of the tautomerism between N3-H and the ureide carbonyl group. In **4e-h** derivatives which contain a thiocarbonyl group, for the weaker electronegativity of the sulfur atom, this tautomerism is not as extensive as in the carbonyl analogs. Thus, the proton on the N3 atom spends most of its time on this atom which is vicinal to the C4 atom and able to couple with its hydrogen. C6-CH_3 and C4-H peaks are indicatives for the presence of the 1,2,3,4-tetrahydropyrimidine ring. The spectral features of **4c**, **4e**, **4f** and **4g** are provided in detail as follows. The characterization data of **4a**, **4b**, **4d** and **4h** have previously been reported. [16,17]

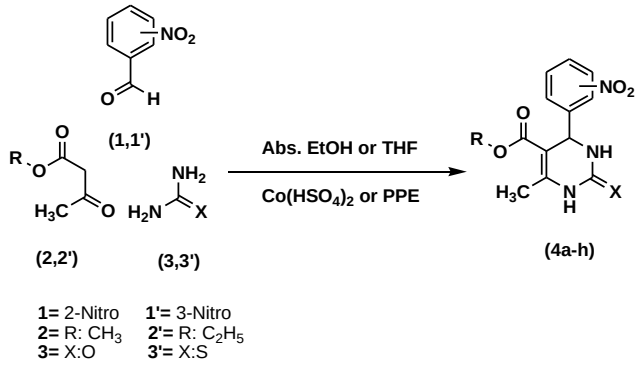

Scheme 1. Synthesis of alkyl-6-methyl-4-[2(3)-nitrophenyl]-2-(thi)oxo-1,2,3,4-tetrahydroprimidine-5-carboxylate **(4a-h)**

*Methyl 6-methyl-4-(3-nitrophenyl)-2-oxo-1,2,3,4-tetrahydroprimidine-5-carboxylate (**4c**)*

Mol. Formula: $C_{13}H_{13}N_3O_5$, Yield: 40%, MW: 291.26 g.mol^{-1}, MP: 280-282 °C, FT-IR (KBr): ϒ (cm^{-1}) 3356,3219 (N-H ureide), 3098 (C-H aromatic), 2959 (C-H aliphatic), 1698 (C=O ester), 1640 (C=O ureide), 1534 (C=C alkene), 1458 (C=C aromatic), ^{1}H-NMR (DMSO-d_6): δ (ppm) 2.28 (s, CH_3-C(6), 3H), 3.54 (s, CH_3COO, 3H), 5.29 (s, H-C(4), 1H), 7.67-8.13 (m, H-C(2),H-C(4),H-C(5), H-C(6) phenyl, H-N(1), 5H), 9.38 (s, H-N(3) , 1H), Mass m/z (%): 290.0 (M-1); Anal. Calcd. (%) for $C_{13}H_{13}N_3O_5$: C, 53.61; H, 4.50; N, 14.43. Found: C, 53.72; H, 4.32; N, 14.71.

*Methyl 6-methyl-4-(2-nitrophenyl)-2-thioxo-1,2,3,4-tetrahydroprimidine-5-carboxylate (**4e**)*

Mol. Formula: $C_{13}H_{13}N_3O_4S$, Yield: 41%, MW: 307.33 g.mol^{-1}, MP: 213.8-215 °C, FT-IR (KBr): ϒ (cm^{-1}) 3243 (N-H ureide), 3176 (C-H aromatic), 3009(C-H aliphatic), 1716 (C=O ester), 1670 (C=S ureide), 1571 (C=C aromatic), 1523 (C=C alkene), 1464 (C=C aromatic), ^{1}H-NMR (DMSO-d_6): δ (ppm) 2.28 (s, CH_3-C(6), 3H), 3.39 (s, CH_3COO, 3H), 5.89 (d, J = 2.8, H-C(4), 1H), 7.48-7.55 (m, H-C(4),H-C(6) phenyl, 2H), 7.42 (t, J = 7.6 Hz, H-C(5) phenyl, 1H), 7.89 (d, J = 8.0 Hz, H-C(3) phenyl, 1H), 9.67 (s, H-N(1) , 1H), 10.48 (s, H-N(3) , 1H), Mass m/z (%): 306.3 (M-1); Anal. Calcd. (%) for $C_{13}H_{13}N_3O_4S$: C, 50.81; H, 4.26; N, 13.67. Found: C, 50.62; H, 4.19; N, 13.81.

*Ethyl 6-methyl-4-(2-nitrophenyl)-2-thioxo-1,2,3,4-tetrahydroprimidine-5-carboxylate (**4f**)*

Mol. Formula: $C_{14}H_{15}N_3O_4S$, Yield: 46%, MW: 321.35 g.mol^{-1}, MP: 219-221 °C, FT-IR (KBr): ϒ (cm^{-1}) 3229 (N-H ureide), 3169 (C-H aromatic), 2987 (C-H aliphatic), 1714 (C=O ester), 1655 (C=S ureide), 1572 (C=C aromatic), 1524 (C=C alkene), 1474 (C=C aromatic), ^{1}H-NMR (DMSO-d_6): δ (ppm) 0.92 (t, J= 7.2 Hz, $C\underline{H}_3CH_2COO$, 3H), 2.29 (s, CH_3-C(6), 3H), 3.84-3.87 (q, J = 6 Hz, $CH_3C\underline{H}_2COO$, 2H), 5.94 (d, J = 2.8 Hz, H-C(4), 1H), 7.49-7.55 (m, H-C(4),H-C(6) phenyl, 2H), 7.75 (t, J = 8.0 Hz, H-C(5) phenyl, 1H), 7.92 (d, J = 8.0 Hz, H-(C3) phenyl, 1H), 9.59 (s, N(1) , 1H), 10.45 (s, N(3), 1H), Mass m/z (%): 320.35 (M-1); Anal. Calcd. (%) for $C_{14}H_{15}N_3O_4S$: C, 52.33; H, 4.70; N, 13.08. Found: C, 52.52; H, 4.39; N, 12.87.

*Methyl 6-methyl-4-(3-nitrophenyl)-2-thioxo-1,2,3,4-tetrahydroprimidine-5-carboxylate (**4g**)*

Mol. Formula: $C_{13}H_{13}N_3O_4S$, Yield: 57%, MW: 307.33 g.mol^{-1}, MP: 251-252 °C FT-IR (KBr): ϒ (cm^{-1}) 3308 (N-H ureide), 3175 (C-H aromatic), 2955 (C-H aliphatic), 1662 (C=O ester), 1566 (C=S ureide), 1531 (C=C alkene), 1459 (C=C aromatic), ^{1}H-NMR (DMSO-d_6): δ (ppm) 2.30 (s, CH_3-C(6), 3H), 3.55 (s, CH_3COO, 3H), 5.32 (d, J = 3.6 Hz, H-C(4), 1H), 7.64-7.69 (m, H-C(5),H-C(6) phenyl, 2H), 8.06 (bs, H-C(2) phenyl, 1H), 8.13-8.16 (m, H-C(4) phenyl, 1H) 9.78 (s, H-N(1), 1H), 10.52 (s, H-N(3), 1H), Mass m/z (%): 306.3 (M-1); Anal. Calcd. (%) for $C_{13}H_{13}N_3O_4S$: C, 50.81; H, 4.26; N, 13.67. Found: C, 50.55; H, 4.05; N, 13.43.

Biology

Cytotoxicity

The cytotoxicities of all compounds were determined by MTT assay. All compounds were tested for cytotoxic properties against HeLa cells. Data are given in Table **2** and Figure **3** in terms of IC_{50} values and cell viability at different concentrations, respectively.

According to Table **2**, the most potent compound in terms of cytotoxicity was **4d** with an IC_{50} value of 193.70 µmol and the weakest one was **4a**. The studied compounds can be ordered as **4d**>**4f**>**4b**>**4g**>**4h**>**4e**>**4c**>**4a** according to their cytotoxic potencies. From this small set of compounds, no accurate structure-activity relationships but the fact of the higher cytotoxic potency of ethyl ester compounds over the methyl ester ones can be concluded.

Table 2. The cytotoxicity results of the studied compounds against HeLa cells in terms of IC_{50} (µmol)

Compd.	4a	4b	4c	4d	4e	4f	4g	4h
IC_{50}	248.75	208.45	245.26	193.70	217.29	204.02	211.71	216.37

Migration assay

The ability of the less cytotoxic compounds (**4a**, **4c**, **4e**, and **4h**) to inhibit cancer cell migration was investigated on 4T1 breast cancer cell line by inexpensive *in vitro* scratch assay. Cells were treated with the compounds at the concentration of 50 µg/mL. The results of this assay are provided in Figure **4**. As shown in this figure, the PBS treated cells exhibited 50 percent wound closure activity. The cells treated with compounds showed inhibition of wound closure in contrast to Nifedipine-treated cells (Nifedipine as the positive control). The anti-migratory effects were more apparent for **4a** and **4e** which were more potent than Nifedipine. However, other compounds did not exhibit any inhibitory effects on the cancer cells migration.

The obtained results demonstrate that some of the prepared compounds which were not cytotoxic could inhibit migration of the breast cancer cells and this fact was more apparent for **4a** and **4e**. Compound **4e** was one of the compounds with high *in silico* affinity, compared to other molecules, to the Fascin binding site.

Docking studies

Molecular docking simulation was performed to investigate the binding mode of the prepared compounds to the Fascin protein. Crystallographic 3D structure of 3LLP was used in docking studies. A blind ligand-protein docking approach was utilized to find the ligand binding site inside the protein. Since the target molecule was too big to be covered by one grid box, four separate grid boxes with different centers were applied for each compound then autodock calculations were run. Based on the results obtained from docking in each grid box, binding site was determined. Nifedipine was docked as the known inhibitor of the Fascin protein.

The results of this part of the study including the estimated free binding energy values (ΔG_{bind}) of the docked positions, expressed in kcal/mol, and the favorable interactions with the key amino acid residues at the active site of Fascin 3D structure are provided in Table **3**. Among the studied compounds **4c**, **4d**, **4e** and **4h** were recognized potent in docking studies in terms of the estimated binding free energy changes and interactions within the Fascin active site. ΔG_{bind} values of the docking poses of these three compounds were within the range of -8.21 to -8.72 kcal/mol, not very different from the binding free energy change for Nifedipine (-9.8 kcal/mol). Molecular interactions of the best docked conformation of Nifedipine are provided in Figure **5**. Figure **6** demonstrates the interactions of **4h**, the most potent compound in terms of *in silico* inhibition of the Fascin protein with the lowest ΔG_{bind} (-8.72 kcal/mol), with the active site residues of Fascin.

The obtained results show that all the docked compounds except **4b** were located in the same biding site as Nifedipine. They formed hydrophobic interactions with almost the same residues inside the binding site as Nifedipine did. The corresponding ΔG_{bind} values were not as high as the ΔG_{bind} of Nifedipine, but can be regarded acceptable for the *in silico* inhibitory potential.

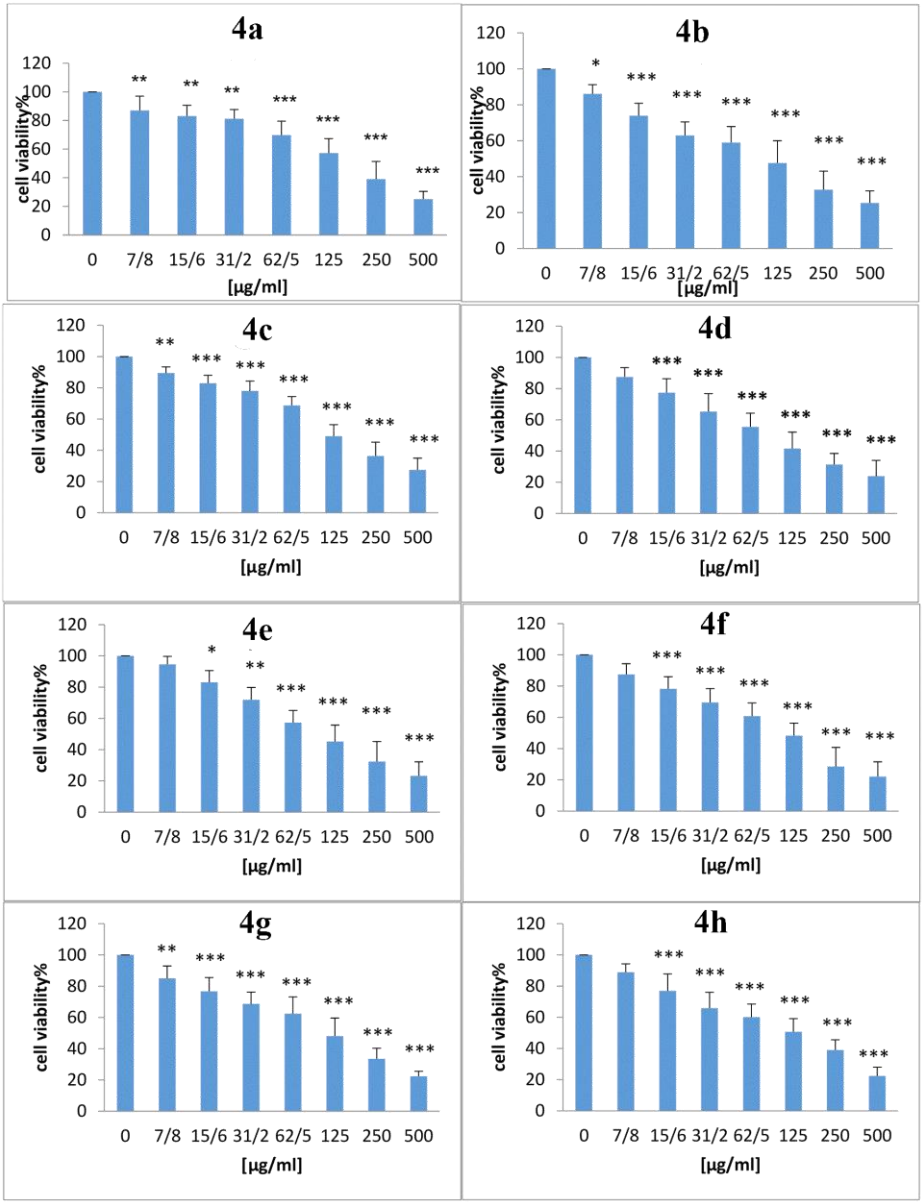

Figure 3. Cytotoxicity results of the studied compounds in terms of cell viability

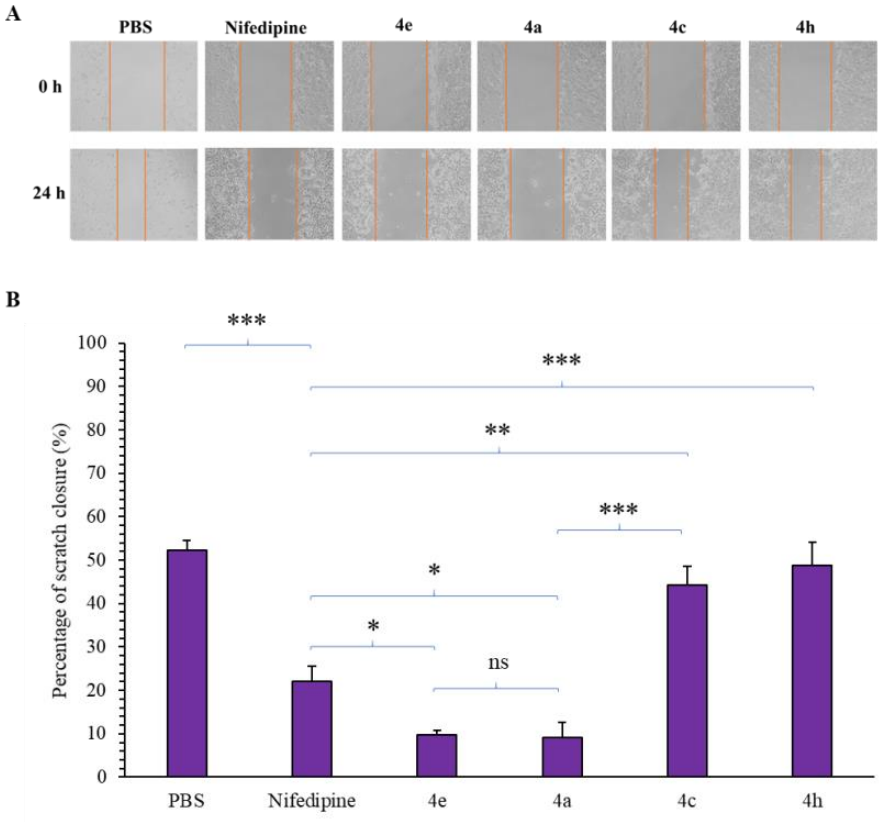

Figure 4. Analysis of the **4a**, **4c**, **4e**, and **4h** ability to inhibit 4T1 cancer cell migration by *in vitro* scratch assay. **A)** The images of the scratched area are acquired at 0 and 24 hours. The orange lines define the areas lacking cells. **B)** Percentage of the scratch area closure after 24 h. (*:P ≤0. 05, **:P ≤0.005 , ***:P ≤0.001 , ns : not significant)

As can be seen in Figures **5**, in the docking simulation of Nifedipine the two oxygen atoms of NO_2 group formed hydrogen bonds with Lys220. The NO_2 oxygens were also involved in electrostatic interactions with this residue. **4h** as the most potent *in silico* inhibitor of Fascin established the same hydrogen bonds and electrostatic interactions in its best docked form inside the binding site. A π–cationic interaction between the nitrophenyl ring and Lys220 was also observed for **4h** which has an important role in fixing the molecule inside the binding site (Figure **6**). These hydrogen bonds and π–cationic interaction were common in all the four most potent compounds. The OCH_3 moieties of 3,5-dicarboxylate esters in Nifedipine formed extra hydrogen bonds with Lys220 and Leu256. The studied compounds lacked the C5 ester group but, the OC_2H_5 moiety of 3-carboxylate ester in **4h** was involved in hydrogen bondng with Lys220. Such an interaction was not observed in other potent compounds; instead, N1-H/N3-H and/or the carbonyl group in C2 position of tetrahydroprimidine ring were involved in some hydrogen bonding with the binding site residues. The dihydropyridine NH hydrogen donated hydrogen to Val10 for a hydrogen bond and N1-H of the tetrahydroprimidine ring of **4h** did the same. None of these interactions were observed for the least potent compound, **4b** with ΔG_{bind} of -5.91 kcal/mol (Table **3**). It is noteworthy that the π–cationic interaction between the nitrophenyl ring and Lys220 compensated the lack of hydrogen bonding.

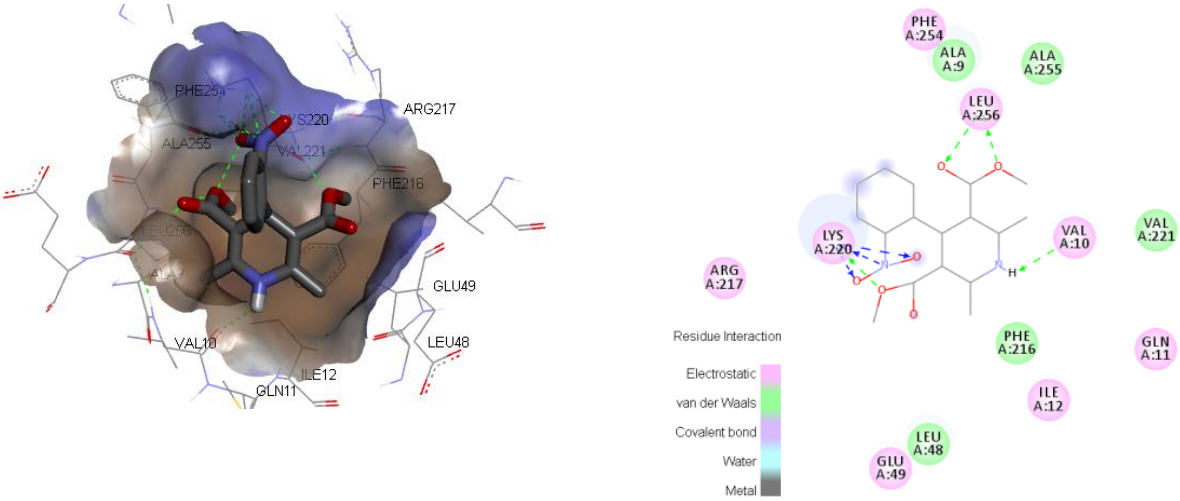

Figure 5. Nifedipine docked inside the Fascin active site. The 3D ligand interaction diagram shows hydrogen bonding (green dashed line) and the 2D diagram demonstrates electrostatic interactions (blue dashed line) of the nitro group with the positively charged residue Lys220.

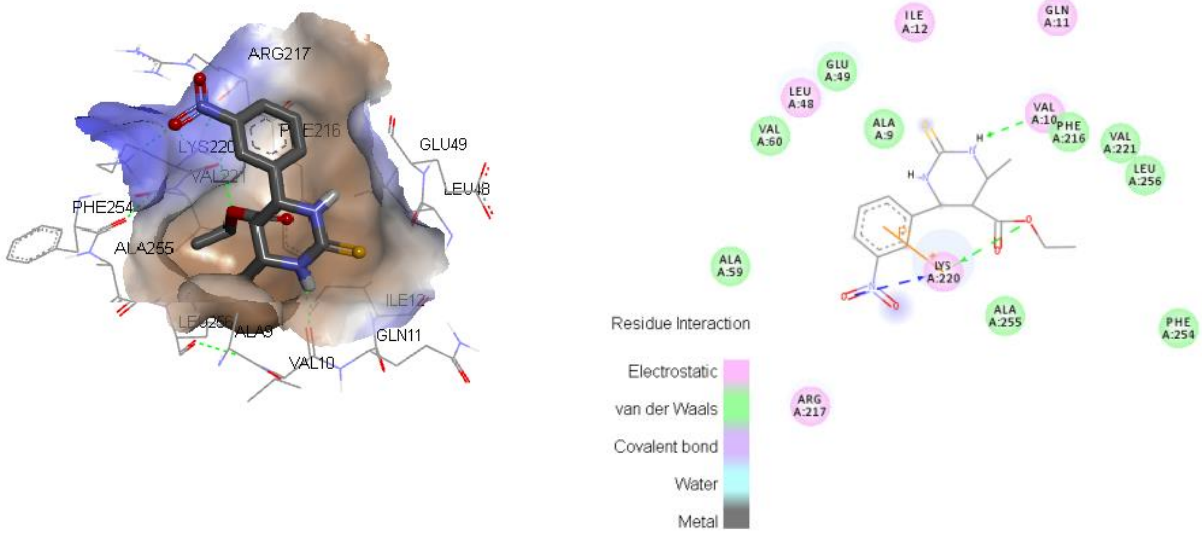

Figure 6. Compound **4h** inside the Fascin binding site. The 3D ligand interaction diagram shows hydrogen bonding (green dashed line) and the 2D diagram demonstrates electrostatic interactions (blue dashed line) of the nitro group with the positively charged residue Lys220.

The most potent compound in terms of migration inhibition, **4e**, had the same interactions with the Fascin binding site as the weakest *in vitro* inhibitor, **4h**. As can be seen in Figure **7** the *ortho* nitro group established electrostatic and hydrogen bonds with

Lys220. Here again, a π–cationic interaction between the nitrophenyl ring and Lys220 was also observed. Other amino acids involved in interactions were almost the same as what was observed for compound **4h** and Nifedipine.

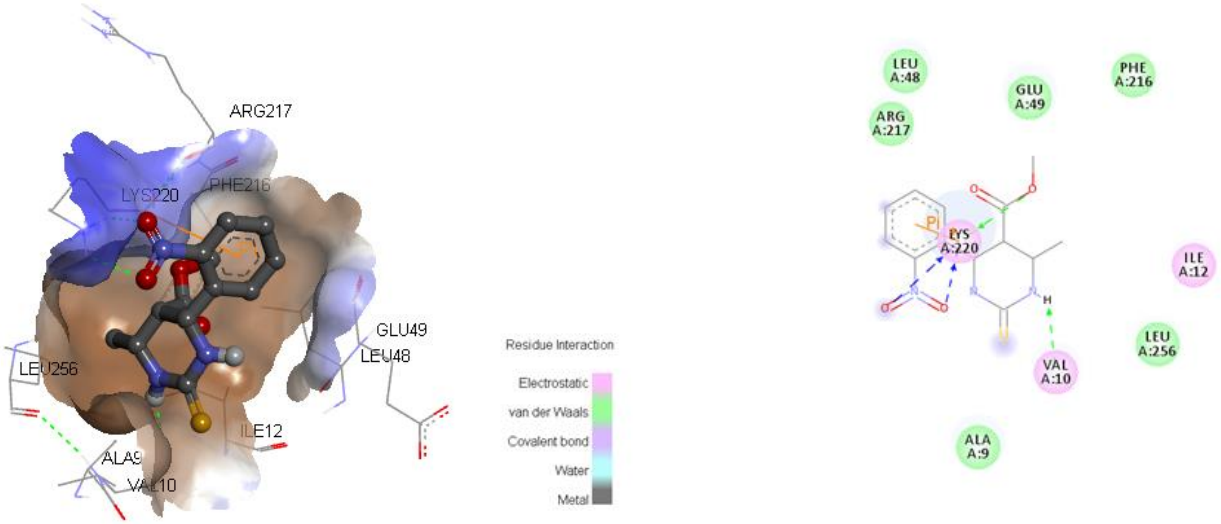

Figure 7. Compound **4e** inside the Fascin binding site. The 3D ligand interaction diagram shows hydrogen bonding (green dashed line) and the 2D diagram demonstrates electrostatic interactions (blue dashed line) of the nitro group with the positively charged residue Lys220. π–cationic interaction is shown with orange lines in both diagrams.

It should be noted that all the studied compounds as well as Nifedipine were docked into the same pocket inside the Fascin protein and the docking results had a high degree of reproducibility according to the clustering histograms in the docking output files. Thus, all the studied compounds were docked into their actual binding site inside the Fascin protein. The reason behind the controversy between the *in vitro* and *in silico* results might be that the scratch assay is not a representative of the inhibition of Fascin and other cellular targets. Theses targets may also be inhibited by some of the studied compounds.

Conclusions

In the present study, it was aimed at the synthesis of a series of alkyl-6-methyl-4-[2(3)-nitrophenyl]-2-(thi)oxo-1,2,3,4-tetrahydroprimidine-5-carboxylates which possess structural features of both Monastrol as an anti-cancer drug and Nifedipine as a Fascin blocker compound. All of the compounds were investigated *in silico* for their ability to inhibit the Fascin protein using molecular docking simulation. It should be considered that in the case of abnormal proliferation of a tissue, if the proliferation is completely inhibited, then there would not be any need to inhibit cell migration. Thus, it seemed to us that the anti-migratory activity would be a good additive feature for moderately active cytotoxic agents. Those cells which were not destroyed by the cytotoxic activity of the compound would not have any chance for migration which leads to invasion. In fact, this feature would change nothing in the process of the solid cancer treatment with a strong cytotoxic agent.

The studied compounds were ordered as **4d**>**4f**>**4b**>**4g**>**4h**>**4e**>**4c**>**4a** according to their cytotoxic potency. The most potent one as a cytotoxic compound was **4d** with an IC_{50} of 193.70 µmol and the weakest one was **4a** (IC_{50}=248.75 µmol). The least cytotoxic compound was one of the strongest compounds in binding to the Fascine binding site according to molecular docking simulation results (ΔG_{bind}= -7.81 kcal/mol). The controversy between the *in vitro* and *in silico* results may cancel the postulation of the involvement of the Fascin inhibition in the migration inhibition. However, the considerable anti-migratory effects of some of the synthesized compounds proved it to be reasonable to perform further *in vivo* experiments to introduce novel inhibitors of tumor metastasis.

Chem. Biodiversity

Table 3. Interactions between the docked 1,2,3,4-tehtrhydropyridine derivatives and fascin binding site residues

Compd.	Amino acid in hydrogen bond	Hydrogen bond		Amino acids in Van der Waals and electrostatic contacts	Amino acid in electrostatic interaction with NO_2	π-cation interaction with Lys2220	ΔG_{bind} (kcal/mol)
		Distance (Å)	θ Angle (°)				
4a	Lys220	1.85	164	Ala9,Ile12,Leu48, Lys220,Val221,	Lys220	$-C_6H_4-NO_2$	-7.81
	Lys220	1.72	158	Phe254,Ala255,Leu256, Phe216			
	Lys220	1.89	120				
4b	Ala7	1.69	160	Ala7,Arg308,Gln295,Trp171,Val169,Pro170, Tyr152	-	-	-5.91
4c	Lys220	1.96	141	Ala9,Val10,Gln11,Ile12,Leu48, Lys220,Leu256	Lys220	$-C_6H_4-NO_2$	-8.34
	Ile12	1.75	123				
	Val10	2.04	138				
4d	Lys220	1.73	158	Val10,Ile12,Leu48,Arg217 ,Lys220,	Lys220	$-C_6H_4-NO_2$	-8.43
	Lys220	1.74	160	Val221,Phe254,Ala255,Leu256			
	Ile12	2.17	168				
4e	Lys220	1.59	161	Ala9,Val10, Leu48,Glu49	Lys220	$-C_6H_4-NO_2$	-8.21
	Lys220	1.68	148	Phe216,Lys220,Leu256			
	Lys220	1.90	163				
	Val10	2.13	135				
4f	Lys220	2.11	136	Ala9,Val10,Ile12,Leu48,Phe216,Lys220, Val221,Ala255,Leu256	Lys220	-	-6.51
4g	Lys220	1.80	130	Ala9,Val10,Gln11,Ile12,Leu48,Glu49, Lys220	Lys220	-	-7.49
	Lys220	1.82	142				
4h	Lys220	1.77	159	Val10,Ile12,Leu48,Phe216 ,Arg217,Lys220, Val221,Leu256	Lys220	$-C_6H_4-NO_2$	-8.72
	Val10	1.94	122				
Nifedipine	Val10	1.90	131	Ala9,Val10, Ile12, Leu48, Phe216,Lys220, Val221,Ala255,Leu256	Lys220	-	-9.8
	Leu256	2.13	161				
	Lys220	2.21	154				
	Lys220	1.80	144				
	Lys220	1.99	148				

Experimental Section

Chemistry

All chemicals, reagent and solvents were obtained from commercial suppliers and were freshly used after purification by standard procedures. Melting points were determined on an Electrothermal 9200 Melting Point apparatus and were uncorrected. ^{1}H-NMR spectra were recorded in DMSO-d_6 on a Bruker-Ultrashield 400MHz spectrometer (Germany). All the chemical shifts were reported as (δ) values (ppm) against tetramethylsilane as an internal standard. IR spectra were recorded with a Perkin Elmer IR spectrophotometer. Electrospray mass spectra (ESI-MS) were obtained in negative and positive ion mode on a SHIMADZU LCMS-2010 EV spectrometer using methanol as solvent, a capillary voltage of 4500 V and a cone voltage of 10 V. All experiments were monitored by analytical thin layer chromatography (TLC) on pre-coated silica gel 60 F254 aluminum plates (Merck, Germany). Suitable names for the compounds were given with the aid of ChemOffice 2014 software. The final products were prepared in 16-61%. Their purity was determined by thin layer chromatography using several solvent systems of different polarities and data obtained from elemental analysis, to an accuracy of within ±0.4%. General procedure for the preparation of the compounds is provided in Scheme **1**.

Synthesis of the Lewis acid catalysts

Cobalt hydrogen sulfate $Co(HSO_4)_2$ was prepared according to the method of Memarian et al.[18] Poly phosphate ester was synthesized using the procedure reported by Kappe and his colleagues.[19]

General procedure for the preparation of Biginelli compounds using cobalt hydrogen sulfate as the catalyst

A mixture of the proper aldehyde (1,1'; 3.0 mmol), methyl (ethyl) aceto acetate ester (2,2'; 3.0 mmol), urea (3, 3.9 mmol) and $Co(HSO_4)_2$ as the Lewis acid catalyst (0.9 mmol) in EtOH (4 mL) was heated at 85 ºC for 24 hours. After the completion of the reaction indicated by thin layer chromatography (TLC) (chloroform:methanol, 10:1), the mixture was cooled down to room temperature and water was added. Stirring was continued for several minutes for dissolving the catalyst and the excess of urea. Solid products (**4a-d**) were filtered and washed with water. Pure products were obtained by recrystallization from ethanol. The chemical structures of the products were characterized by spectroscopic data of IR and ^{1}H-NMR.

General procedure for the synthesis of Biginelli compounds using poly phosphate ester as the catalyst

A mixture of the proper aldehyde (1,1'; 1 mmol), methyl (ethyl) aceto acetate ester (2,2'; 1.0 mmol) and thiourea (3', 1.5 mmol) was added to a solution of polyphosphate ester (150 mg) in tetrahydrofurane (4 mL) then refluxed for 17 hours. The reaction progress was monitored using TLC until the reactants disappeared in the reaction mixture. Then it was cooled down to room temperature and some crushed ice was added. After stirring for some more hours the resulted precipitate was filtered off, washed with cold water and dried in a vacuum oven for 24 hours to give dry **4e-h**.

Biology

Cell Culture

HeLa and 4T1 cell lines were purchased from Pasteur Institute, Iran. Cells were maintained in RPMI-1640 afforded with 10 % (v/v) fetal bovine serum (FBS) and Penicillin/Streptomycin (50 IU/ml, 50 mg/ml) at 37 °C in a humidified atmosphere containing 5% CO_2.

In vitro cytotoxicity assay

The cytotoxicity assay of the selected compounds was performed against HeLa cell line according to a previously reported method.[20] HeLa cells were sub-cultured regularly via Trypsin/ethylene diamine tetra-acetic acid (EDTA). To evaluate the cell viability, a test with 3-(4,5-dimethylthiazole-2-yl)-2,5-diphenyl tetrazolium bromide (MTT) assay was performed. MTT is reduced to

formazan crystals in the mitochondria of viable cells, and when the crystals are dissolved in DMSO they produce a dark-purple color. Briefly, HeLa cells were plated in 96-well plates and grown overnight. Then cells were exposed to serial concentrations of selected compounds (7.8–500 µg/mL) and incubated at 37°C for 48 h. At the end of the incubation time, 20 µL of MTT solution (5 mg/mL) was added and incubated for further 3 hours. The medium containing unreacted MTT was removed. Subsequently, 15 mL of DMSO was added to each well to dissolve the formazan crystals. Finally, the absorbance of the dissolved formazan was measured at 540 nm in an Enzyme-Linked Immuno Sorbent Assay (ELISA) reader. All the experiments were performed in duplicate. Statistical analyses were achieved using the SPSS software package (v.17). One-way ANOVA tests and TukeyPost Hoc test were used with a confidence level of 0.05 to assess the statistically significant homogeneous subsets. IC_{50} values were calculated using GraphPad Prism software.

Migration assay

Convenient and inexpensive *in vitro* scratch assay reported by Liang and his colleagues was employed in this research for analysis of cell migration.[21] The 4T1 cancer cells were seeded into 12-well culture plates at a 5 × 105 cells/mL concentration and cultured overnight prior to serum starvation for 24 hours. The cell monolayers were then incubated with 10 mg/mL of Mytomycin C to stop cell proliferation. The monolayers were carefully wounded using a pipette tip and washed three times with PBS to remove detached cells. The wounded monolayers were then incubated for 24 hours with Nifedipine, **4c**, **4a**, **4e**, and **4h** at the same concentrations (50 µg/mL). The wounds photographs were taken at the onset of the test, when the scratch was made and after 24 hours. Cell migration was exhibited as the percentage of scratch closure according to borders (orange lines) closing.

Molecular docking studies

In order to gain some insight into the binding mode of the newly designed compounds with Fascin protein, it was decided to focus on the inhibition of this protein by carrying out molecular docking studies. Crystallographic structure of Fascin was retrieved from the RCSB protein Data Bank, PDB code: 3LLP. The docking studies were performed using AUTODOCK 4.2 software package, with the implemented empirical free energy function and the Lamarckian genetic algorithm (LGA).[22]

Ligand preparation

For ligand preparation, three-dimensional structures of the compounds were constructed and optimized using the Polak-Ribiere conjugate gradient algorithm and PM3 semi-empirical method implemented in Hyperchem software. These optimized structures were used as inputs of the Auto Dock tools. Then the partial charges of atoms were calculated using the Gasteiger-Marsili procedure implemented in the Auto Dock tools package.[23] Non-polar hydrogens of the compounds were merged and then rotatable bonds were assigned. PDB format of this ligand was converted to PDBQT file to generate atomic coordinates.

Protein preparation

All irrelevant hetero atoms including water molecules were removed from the crystal structure using notepad software. All missing hydrogens were added, and after determining the Kolman united atom charges, non-polar hydrogens were merged into their corresponding carbons using Auto dock tools. As the final part of the process of the protein preparation, desolvation parameters were assigned to protein atom.

Molecular docking simulation

Using Auto grid implemented in the Auto dock program, the grid maps were calculated. Since the target molecule was too big to be covered by one grid box, four separate grid boxes with different centers were applied for each compound then autodock calculations were run. Based on the results obtained from docking in each grid box, binding site was determined. Then a grid box was chosen to be large enough to contain the determined binding site of the protein and the significant regions of the surrounding surface. The grid map of 126×126×126 points and a grid point spacing of 0.375 Å (roughly a quarter of the length of a carbon-carbon single bond) were applied using the Autogrid. The Lamarckian Genetic Algorithm (LGA) approach was selected as the search algorithm for the

global optimum binding position search provided by Autodock 4.2. For the LGA method, 100 independent docking runs were carried out for each atom. An initial population of random individuals with a population size of 150 individuals was considered. For investigation of hydrogen bonding and π–π stacking interactions which are established through the docking procedure AutoDockTools and DS Visualizer 3.5 software were utilized.

Acknowledgment

The authors would like to thank the School of pharmacy, Isfahan University of medical science, Isfahan, Iran for financing this project.

Author Contribution Statement

This article was extracted from the PharmD research project of Narges Riahi. She performed all the synthesis procedures by herself and the biological assays with the help of Amirhosein Kefayat and Ahmad Ghasemi. Mohammadhosein Asgarshamsi wrote some parts of the article and prepared the solutions for migration inhibition assay. Afshin Fassihi was the supervisor of the chemistry part of the research and Mojtaba Panjehpoor was the supervisor of the biological part of the project.

Conflicts of interest

There are no conflicts of interest in this report.

References

[1] A. F. Chambers, A. C. Groom AC, I. C. MacDonald, 'Metastasis: dissemination and growth of cancer cells in metastatic sites', *Nat. Rev. Cancer* **2002**, *8*, 563-572.

[2] M. S. Wong, S. M. Sidik, R. Mahmud, J. Stanslas, 'Molecular targets in the discovery and development of novel antimetastatic agents: current progress and future prospects', *Clin. Exp. Pharmacol. Physiol* **2013**, *5*, 307-319.

[3] J. E. Talmadge, I. J. Fidler, 'AACR centennial series: the biology of cancer metastasis: historical perspective', *Cancer Res* **2010**, *14*, 5649-5669.

[4] P. K. Mattila, P. Lappalainen, 'Filopodia: molecular architecture and cellular functions', *Nat. Rev. Mol. Cell Biol* **2008**, *6*, 446-454.

[5] S. Yang, F. K. Huang, J. Huang, S. Chen, J. Jakoncic, A. Leo-Macias, R. Diaz-Avalos, L. Chen, J. J. Zhang, X. Y. Huang, 'Molecular mechanism of Fascin function in filopodial formation', *J. Biol.Chem* **2013**, *1*, 274-284.

[6] D. Vignjevic, S. I. Kojima, Y. Aratyn, O. Danciu, T. Svitkina, G. G. Borisy, 'Role of Fascin in filopodial protrusion', *J. Cell Biol* **2006**, *6*, 863-675.

[7] A. Grothey, R. Hashizume, A. A. Sahin, P. D. McCrea, 'Fascin, an actin-bundling protein associated with cell motility, is upregulated in hormone receptor negative breast cancer', *Br. J. Cancer* **2000**, *7*, 870-873.

[8] N. Kureishy, V. Sapountzi, S. Prag, N. Anilkumar, J. C. Adams, 'Fascins and their roles in cell structure and function', *Bioessays* **2002**, *4*, 350-361.

[9] L. Chen, S. Yang, J. Jakoncic, J. J. Zhang, X. Y. Huang, 'Migrastatin analogues target Fascin to block tumour metastasis', *Nature* **2010**, *7291*, 1062-1066.

[10] R. Kraft, A. Kahn, J. L. Medina-Franco, M. L. Orlowski, C. Baynes, F. López-Vallejo, K. Barnard, G. M. Maggiora, L. L. Restifo, 'A cell-based Fascin bioassay identifies compounds with potential anti-metastasis or cognition-enhancing functions', *Dis. Model Mech* **2013**, *1*, 217-235.

[11] S. Sepehri, H. P. Sanchez, A. Fassihi, 'Hantzsch-type dihydropyridines and Biginelli-type tetra-hydropyrimidines: a review of their chemotherapeutic activities', *J. Pharm. Pharm. Sci* **2015**, *1*, 1-52.

[12] B. Lokeshwar, H. Escatel, B. Zhu, 'Cytotoxic activity and inhibition of tumor cell invasion by derivatives of a chemically modified tetracycline CMT-3 (COL-3)', *Curr. Med. Chem* **2001**, *3*, 271-279.

[13] A. Gandalovičová, D. Rosel, M. Fernandes, P. Veselý, P. Heneberg, V. Čermák, L. Petruželka, S. Kumar, V. Sanz-Moreno, J. Brábek, 'Migrastatics- anti-metastatic and anti-invasion drugs: promises and challenges', *Trends Cancer* **2017,** *6*, 391-406.

[14] Y. Hu, X. Bi, P. Zhao, H. Zheng, X. Huang, 'Cytotoxic Activities, SAR and anti-invasion effects of butylphthalide derivatives on human Hepatocellular carcinoma SMMC7721 Cells', *Molecules* **2015**, *11*, 20312-20319.

[15] P. Biginelli, 'Aldehyde-urea derivatives of aceto- and oxaloacetic acids', *Gazz. Chim. Ital* **1893**, *23*, 360–413.

[16] N. Stiasni, C. O. Kappe, 'A tandem intramolecular Michael-addition/elimination sequence in dihydropyrimidone to quinoline rearrangements', *Arkivoc* **2002**, *8*, 71-79.

[17] N. S. Begum, D. E. Vasundhara, 'Ethyl 6-methyl-4-(3-nitrophenyl)-2-thioxo-1,2,3,4-tetrahydropyrimidine-5- carboxylate', *Acta Cryst. E: Struct Rep Online* **2006**, *62*, o5796-o5798.

[18] H. R. Memarian, M. Ranjbar, 'Synthesis of Biginelli compounds using cobalt hydrogen sulfate', *J. Chinese Chem. Soc* **2011**, *58*, 522-527.

[19] C. O.Kappe, S. F. Falsone, 'Polyphosphate ester-mediated synthesis of dihydropyrimidines. Improved conditions for the Biginelli reaction', *Synlett* **1998**, *7*, 718-720.

[20] F. Ghahremani, D. Shahbazi-Gahrouei, A. H. Kefayat, H. Motaghi, M. A. Mehrgardi, S. Haghjooy Javanmard, 'S1411 aptamer conjugated gold nanoclusters as a targeted radiosensitizer for megavoltage radiation therapy of 4T1 breast cancer cells', *RSC Adv* **2018**, *8*, 4249-4258.

[21] C. C. Liang, A. Y. Park, J. L. Guan, '*In vitro* scratch assay: a convenient and inexpensive method for analysis of cell migration *in vitro*', *Nat. Protoc* **2007**, *2*, 329-333.

[22] G. M. Morris, D. S. Goodsell, R. S. Halliday, R. Huey, W. E. Hart, R. K. Belew, A. J. Olson, 'Automated docking using a Lamarckian genetic algorithm and an empirical binding free energy function', *J. Comput. Chem* **1998**, *14*, 1639-1662.

[23] J. Gasteiger, M. Marsili, 'Iterative partial equalization of orbital electronegativity - a rapid access to atomic charges', *Tetrahedron* **1980**, *22*, 3219-3222.

10.1002/cbdv.201800339

Chem. Biodiversity

Graphical Abstract